EXPERIMENTAL DETERMINATION OF THE REVERSE FLOW ONSET IN A CENTRIFUGAL IMPELLER

by

Jean Paul Barrand

Professor and Chief

Laboratoire de Mécanique de l'E.N.S.A.M. (Lille)

Guy Caignaert

Laboratoire de Mécanique, E.N.S.A.M. (Lille)

Richard Canavelis

Head, Hydraulics Department

Bergeron S.A.—Paris

and

P. Guiton, Retired

Bergeron S.A.

Paris, France

Jean Paul Barrand graduated from the Institut National des Sciences Appliquees de Lyon in 1961. His teaching activities include gas dynamics, thermal engineering and turbomachinery at I.N.S.A. until 1983.

His main research contributions are in the field of shock tube applications, homogeneous condensation and turbomachinery.

Mr. Barrand is now Professor and Chief of the Laboratoire de Mécanique de l'E.N.S.A.M. in Lille, France.

Guy Caignaert graduated from Ecole Nationale Superieure d'Arts et Metiers in 1969. He did his thesis in Fluid Mechanics at the University of Lille in 1978. The subject area was cavitation on the volute tongue of a centrifugal pump.

Mr. Caignaert teaches Mechanics at Ecole Nationale Superieure d'Arts et Metiers (E.N.S.A.M. Lille). His teaching area is in the strength of materials and applied thermodynamics.

Mr. Caignaert's research area is the interactions between impeller and volute (or diffusor) in centrifugal pumps and fans.

Richard Canavelis received his engineering diploma in 1962 from Ecole Centrale de Paris.

From 1962 to 1967, he was a Research Engineer in the Turbomachinery Department of Electricite de France, Direction des Etudes et Recherches.

In 1967, Dr. Canavelis completed his Science Doctorate thesis on Cavitation Erosion in Turbomachinery.

Since 1968, Dr. Canavelis has been an engineer at Bergeron, S.A. and is presently Head of the Hydraulics Department.

ABSTRACT

The importance of problems related to machines operating at partial flow rate led the Société Hydrotechnique de France (S.H.F.) to form a working group on the subject.

In order to better understand partial flow phenomena and to validate flow calculations and correlations, this group has defined an experimental program, the main results of which are presented in this paper.

A low specific speed, 7 bladed impeller was designed. Two different size similar pump models were then manufactured for experiments with water (outlet diameter 354 mm) and air (outlet diameter 517 mm).

The paper gives test results issued from flow visualization and measurements of various quantities varying with flow rate.

Flow visualizations were made in the inlet and outlet regions of the impeller using threads, smoke and cavitation.

A determination of the critical flow rate at the inlet and outlet was also made using the measurements of: pump power input, mean and fluctuating wall pressures, mean and fluctuating velocities (with directional probes, laser velocimeter, and hot wires).

The influence of the variations of some parameters has been examined:

- comparison of vaneless and 6 vanes diffuser,
- effect of a diffuser width modification,
- influence of variable leakage flow rate,
- comparison of results obtained with water and air.

These results were finally compared with correlations available in the technical literature and were used to validate the computer programs developed.

INTRODUCTION

In the division "Engineering Applied Fluid Mechanics" of the Societe Hydrotechnique de France, a working group was created five years ago to study the performance of uncompressible flow turbomachinery in partial flow operating range.

The working group was composed of various people from universities, research centers, pump manufacturers or pump user companies.

This subject proved to be of high interest for manufacturers as well as for users who have met in recent years to report on more and more cases of flow instabilities and mechanical troubles in pumping installations where very low flow rates are reached.

Such problems were encountered in thermal and nuclear power plants during partial load operation as well as in storage plants where important level variations were met.

Among the various projects undertaken by the working group, emphasis was placed on finding a method for the prediction of the reverse flow onset.

It was decided to follow two different paths of research: on one hand by providing flow calculations in the impeller, and on the other hand by using correlations. It was well known that the flow calculations corresponding to low flow rate were very complex because of the presence of viscous phenomena, detachment zones and secondary flows in the hydraulic channels of the impeller. This method of prediction appeared to be a very difficult task. On the other hand, the use of general prediction formulas, as presented in the literature, proved often to be inaccurate when applied to pump design different from those used to establish these correlations [1,2].

In both cases it was necessary to make experimental observations in order to validate the theoretical results. Some of the experimental results found by the working group are presented in this paper.

EXPERIMENTAL SET UP

Impeller Design

The impeller shown in Figure 1 was designed by Neyrpic. It is a rather conventional design whose main data are:

- outlet diameter D_2 = 400 mm
- outlet width b_2 = 30.0 mm
- inlet diameter D_1 = 220.2 mm
- number of blades Z_r = 7
- outlet blade angle β_{2b} = 22°30′
- mean blade thickness e = 7.0 mm
- nominal speed of rotation N = 1200 rpm (ω = 125.66 rad/s)
- nominal flow rate (water) Q_n = 0.112 m^3/s
- total head (water) H_n = 31 m

This gives the following nondimensional quanitities:

- flow coefficient

$$\varphi = \frac{Qn}{2\pi R_2^2 b_2 \omega} = 0.118$$

- head coefficient

$$\psi = \frac{gHn}{\omega^2 R_2^2} = 0.481$$

- specific speed

$$\Omega_s = \frac{\omega(Qn)^{1/2}}{(gHn)^{3/4}} = 0.577$$

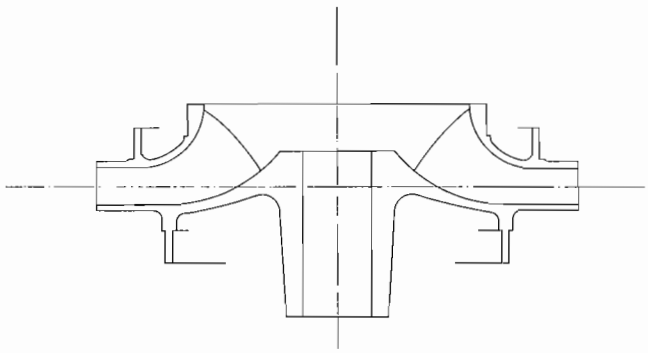

Figure 1. View of Impeller.

Impellers for tests in water and air

Two impellers, geometrically similar to each other and corresponding to the design defined above, were cast in bronze. Table 1 gives the main dimensions of those impellers: the size of the water-impeller was chosen to be adapted easily to the existing test-rig of INSA (in Lyon), the air-impeller was chosen as large as possible taking into account speed of rotation, available power, and desired Reynolds and Mach numbers.

The main results of a dimensional check made on both of the impellers are given in Table 2.

Water Test-rig

Experiments were made on the INSA pump test-rig, a general view of which is shown on Figure 2. The suction pipe had a straight length of 1.40 m. The suction pipe and casing suction side were made of Perspex (Figure 3). The flow rate was measured by means of a venturi with piezometric tubes. The

Table 1: Impellers Operating Data.

Fluid	Outlet diameter D_2 (mm)	Speed of rotation N(r.p.m.)	Reynolds number $Re = (\omega R_2^2)/\nu$	Mach number $M = (\omega R_2)/a$
			$\nu = 1.0 \times 10^{-6}$ m^2/s	
Water	354.4	1100	$Re = 3.61 \times 10^6$	
			$\nu = 0.15 \times 10^{-4} m^2/s$	a = 340 m/s
Air	516.80	2500	$Re = 1.17 \times 10^6$	M = 0.197
		2000	$Re = 9.33 \times 10^5$	M = 0.158
		1700	$Re = 7.93 \times 10^5$	M = 0.134

Table 2: Impellers Dimensions.

Fluid	D2 (mm)		D1 (mm)		b2 (mm)		β_{2b}		e	
	Design	Measured	Design	Measured	Design	Measured	Design	Measured	Design	Measured
Water	354.4	354.56	195.1	195.1	26.58	26.78	22°30′	21°39′	6.20	5.6
Air	516.80	516.80	284.5	284.5	38.76	38.70	22°30′	21°51′	9.04	8.3

total head was measured in sections A and B (Figure 4) by use of two validyne pressure transducers according to the pump test codes (these transducers were calibrated with a mercury manometer).

The pump was driven by a 45 kW D.C. motor with a free floating stator for torque measurement. The speed of rotation was permanently recorded from an optical gauge.

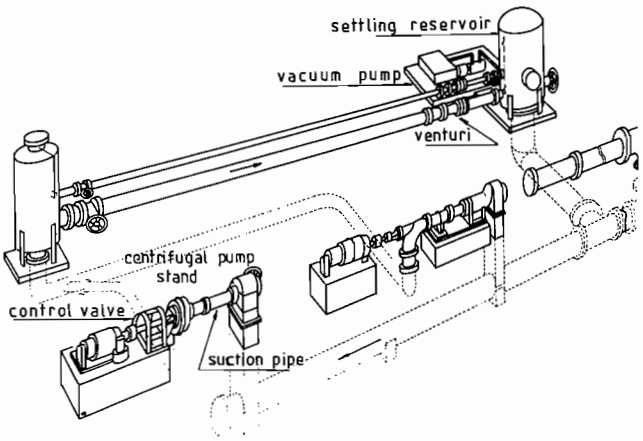

Figure 2. Scheme of Water Test Rig.

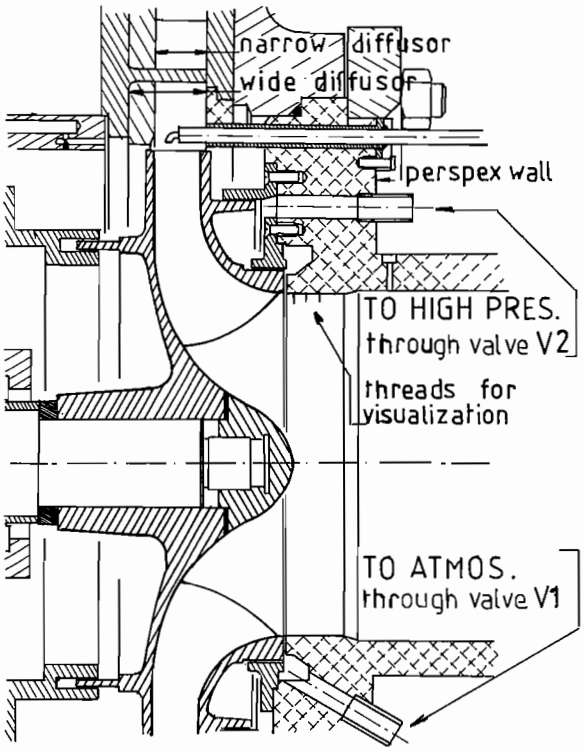

Figure 3. Water Impeller with Leakage Flow Control Device.

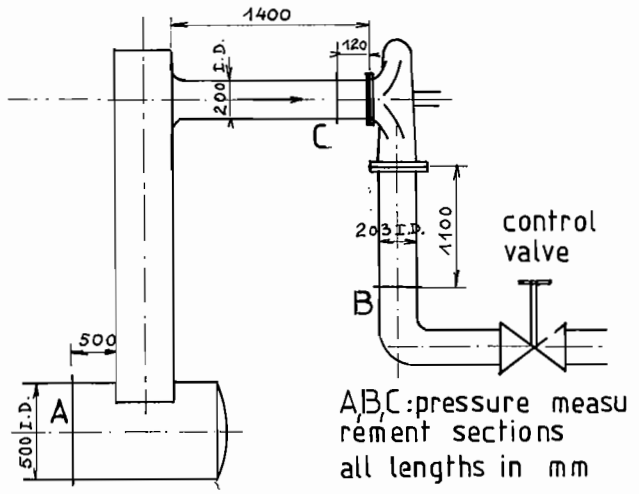

Figure 4. Location of Pressure Measuring Sections in Water Test Rig.

Air Test-rig

The larger impeller was tested in air in an open test-rig. The impeller was driven by a D.C. motor dynamometer whose speed could be varied up to 3000 rpm.

The main dimensions of the casing are shown in Figure 5.

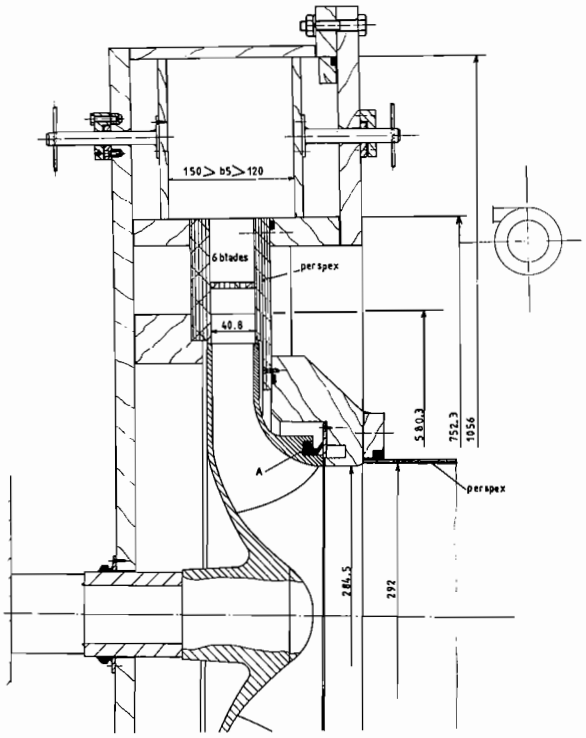

Figure 5. View of Air Test Pump.

As can be seen, the impeller was fitted to a vaned-diffuser (6 blades) geometrically similar to the water diffuser. The diffuser was set up in a volute of uniform cross-section the width of which could be varied.

It must be noticed that seal A (Figure 5) was removed during the measurements reported here.

A schematic description of the test-rig is given in Figure 6. The performance of the "pump" was been determined from the following measurements:

- ambiant conditions (pressure, temperature, relative humidity),
- pressure difference between pump inlet and pump outlet,
- temperature measurement at pump outlet,
- pressure difference at orifice plate for flow measurement,
- speed of rotation and shaft torque.

The flow rate was measured with an orifice plate according to AFNOR or ISO standards [3, 4]. For a given rotation speed, and for each position of the flow control device, all the measurements were recorded and checked with a micro-computer.

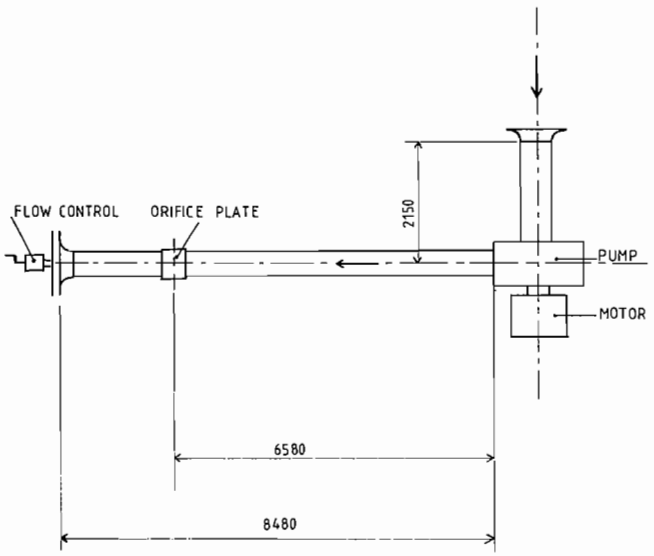

Figure 6. Scheme of Air Test Rig.

Performance Curves

Overall performance results for water and air are given in Figures 7 and 8; the performance was translated into the design dimensions defined in the *Impeller Design* section.

It must be noticed that the power input curves corresponding to the tests in air were corrected by deducting estimated disc friction losses.

The best overall efficiency points were obtained for flow rates at about 0.090 m^3/s in water and 0.075 m^3/s in air.

These values were much lower than the impeller design flow rate (0.112 m^3/s). This difference came essentially from the mismatch between the impeller and diffuser. So that in the present paper, the critical rate of flow is related to the impeller nominal rate of flow and not to the BEP rate of flow.

VISUALIZATIONS

Experimental Devices

In water tests, as shown on Figure 3, threads were stuck on the wall of the suction pipe immediately upstream of the impeller. Visualizations were also made on one impeller blade leading edge by means of video recording of threads or cavitation figures. Threads were also fastened between the impeller

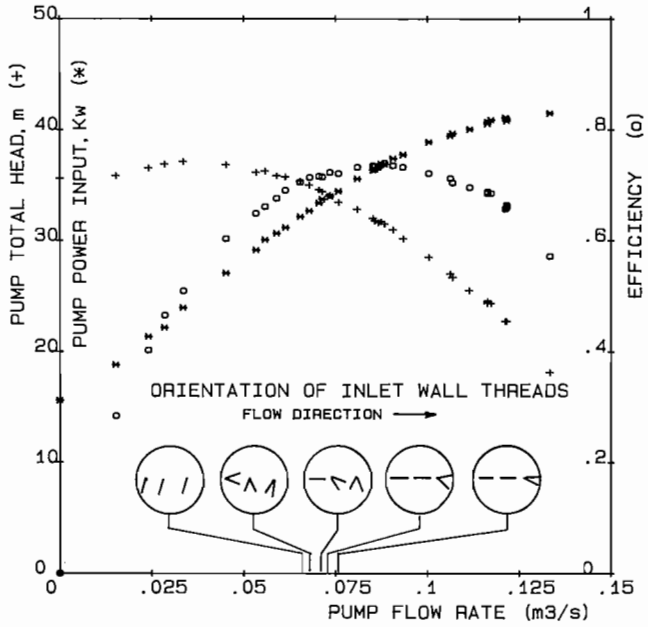

Figure 7. Water Test Pump Performance Curves (Narrow Diffuser).

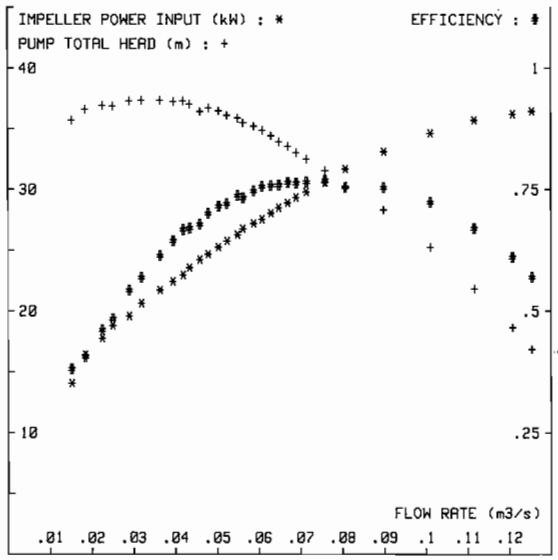

Figure 8. Air Test Pump Performance Curves.

outlet and the diffuser blade inlet diameter on rods (at a diameter of 365 mm). Each rod held two threads, with each one being situated at 5 mm from the front or back wall of the diffuser.

In air, wool threads and a smoke generator were used to visualize flow in the suction pipe in front of the impeller inlet. With both techniques, the probe was introduced across the inlet tube and could be moved radially and axially. At the impeller outlet, only threads were used. A rod on which four threads were fastened (Figure 9) was placed through the diffuser passage inlet.

Results

In every case, the reverse flow at the impulse inlet was initiated by large fluctuations of flow direction, followed by a very stable reverse flow (Figure 7).

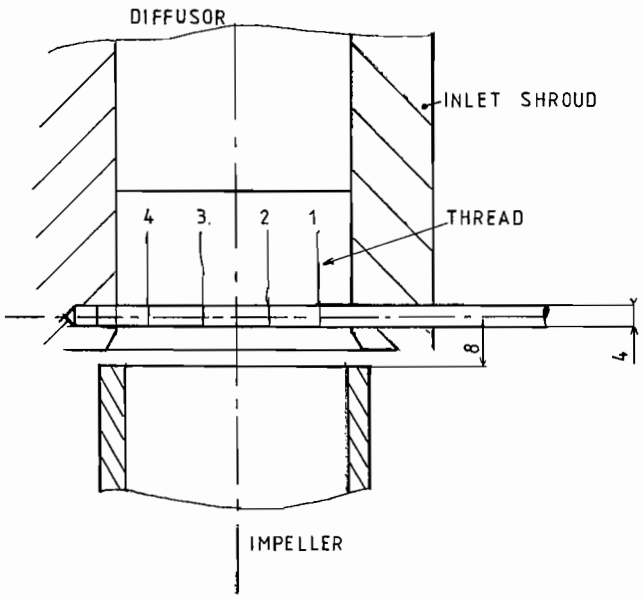

Figure 9. Location of Visualisation Threads at Impeller Outlet (Air Tests).

Results of the traverses in air are given in Figure 10 which shows the position of reverse flow onset points in the inlet pipe for various flow rates lower than the critical one. This map firmly established that reverse flow occured at the inlet blade tip.

At the impeller outlet, the threads were rather parallel at the nominal conditions. When decreasing the flow rate, the angle of the threads with the tangential direction decreased. Suddenly, thread Number 1 (Figure 9) became more tangential than the others and soon began to oscillate, turning from time to time towards the impeller. This indicated the onset of a reverse flow near the impeller front shroud, at the impeller outlet and/or in the diffuser.

Table 3 summarizes the reverse flow detection in water and air at the impeller inlet and outlet.

Table 3. Values of Critical Flow Rate from Visualization Tests.

	Q_K (inlet)/Q_N	Q_K (outlet)/Q_N
Air tests at 2500 rpm	0.67	from 0.78 to 0.81
Water tests at 110 rpm	0.66	from 0.68 to 0.72

The critical rate of flow, Q_K, in the impellers was determined from an estimation of leakage flow coming from the inlet labyrinth. In air tests, a correction was made to take into account the absence of seal A (Figure 5). A labyrinth seal has been made to reduce and control the inlet leakage flow.

CRITICAL FLOW RATE DETECTION FROM PHYSICAL MEASUREMENTS

In cases where visualization was not possible, the critical flow rate could be determined by using measurements of various quantities related to pump performance.

Pump Power Input and Theoretical Head

The critical flow rate could be obtained by using the pump power input curves, according to a method described by Rey, et al. [5]. For each flow rate, the pump power input, corrected with mechanical and disk friction losses, gave the head input, H_i. Then, a curve could be drawn showing the evolution of H_i as a function of the impeller flow rate Q. The deviation of this curve from the theoretical head input, H_{ith}, (without reverse flow) gave an estimation of a critical flow rate (Figures 11a and

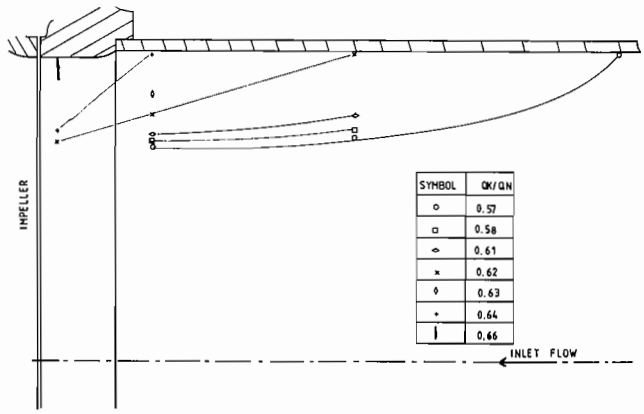

Figure 10. Values of Critical Flow Rate in Inlet Duct (Air Tests).

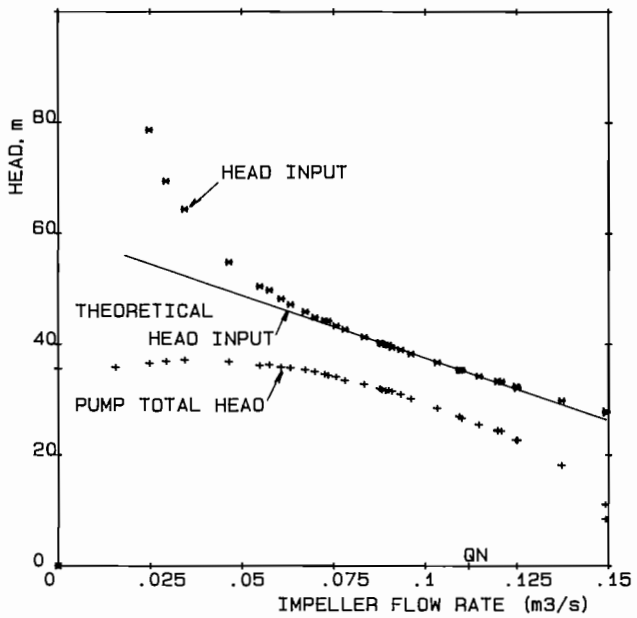

Figure 11a. Determination of Critical Flow Rate from Theoretical and Actual Impeller Head Input (Water Tests).

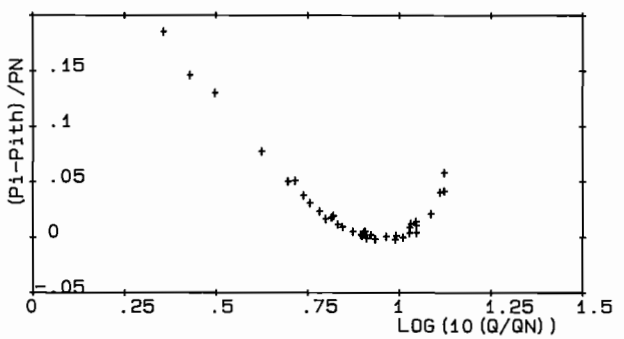

Figure 11b. Determination of Critical Flow Rate from Theoretical and Actual Impeller Power Input (Water Tests).

12a). One could also draw the corresponding dissipation power curves as a function of the logarithm of Q_I/Q_N (Figures 11b and 12b).

However, this method did not appear as a precise criterium for reverse flow onset detection in this case.

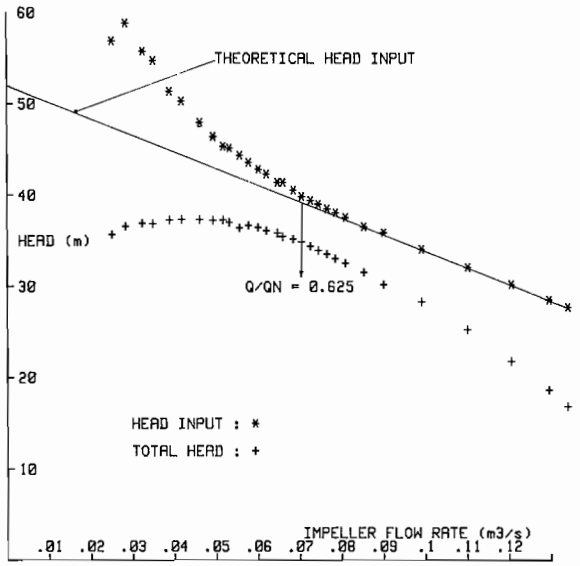

Figure 12a. Determination of Critical Flow Rate from Theoretical and Actual Impeller Head Input (Air Tests).

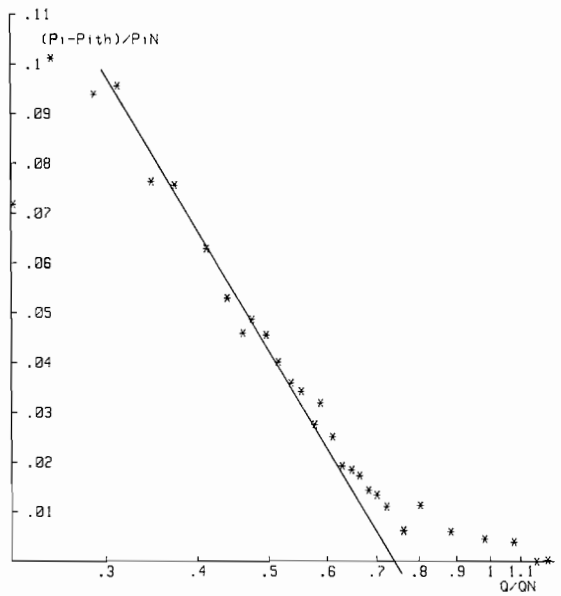

Figure 12b. Determination of Critical Flow Rate from Theoretical and Actual Impeller Power Input (Air Tests).

Static Wall Pressure in the Suction Pipe

After the onset of the reverse flow, a swirling flow of large amplitude took place in the suction pipe and at the modified wall static pressures at sections near the impeller.

The evolution of the pressure difference between the measuring section A (Figure 4) and the measuring section C located 12 cm upstream of the impeller eye, is shown on Figure 13 versus flow rate. From that curve, the relative critical flow rate in the measuring section C would be equal to 0.58. It could then be concluded that the relative critical flow in the impeller was higher than 0.58.

Similar analysis for the instantaneous wall pressure is in progress in the water test-rig.

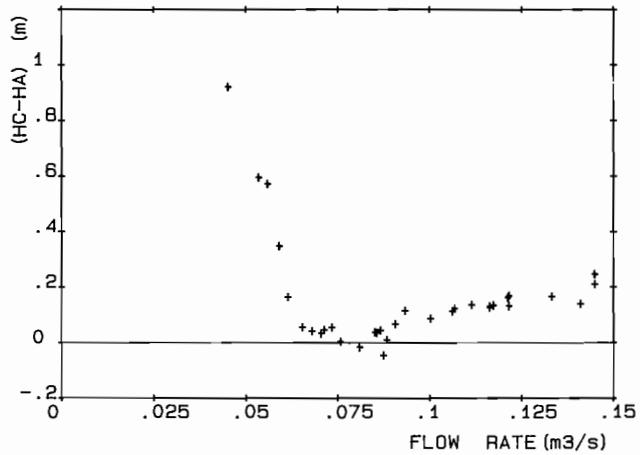

Figure 13. Wall Static Pressure Variations at Impeller Inlet (Water Tests).

Instantaneous Static Pressure at Diffuser Inlet (Air Tests)

A piezo-resistive pressure transducer was put on the front shroud of the diffuser, at about 8 mm from impeller outlet. A frequency analysis of pressure fluctuations was made using a FFT analyser. The evolution of the pressure fluctuation amplitudes, at the impeller blade passing frequency and twice the blade passing frequency when the flow rate was varied (at constant speed of rotation), is shown in Figure 14. At partial flow, for a relative flow rate of about 0.64, the ratio of both amplitudes passed through a sharp maximum, showing a sudden variation of the signal.

Instantaneous Velocity Measurements

Laser Velocimetry in Water Test

A one component Doppler laser velocimeter was used to

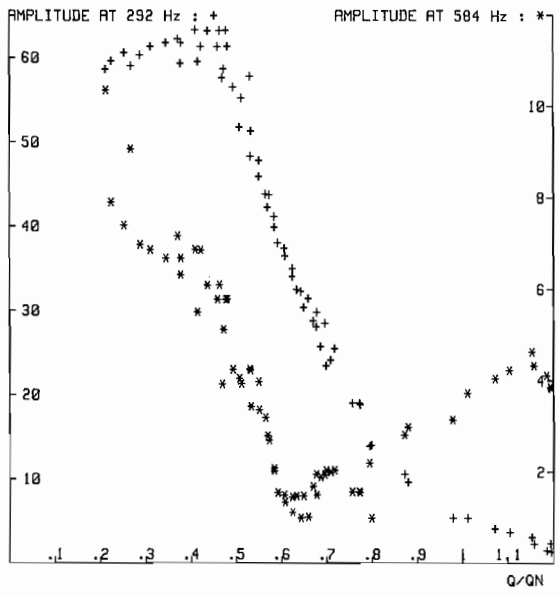

Figure 14. Pressure Fluctuation Analysis at Impeller Outlet with Bladed Diffuser (Air Tests).

measure the instantaneous velocities. The Doppler signal, detected by retrodiffusion, was treated by a digital counter. Simultaneously, the impeller angular position was measured by an optical encoder delivering 1024 points per revolution. Both the velocity component and the angular position entered the central memory of the microcomputer used for the signal treatment.

The radial and peripheral components of velocity were successively recorded at the impeller outlet, 4 mm downstream from the outlet diameter, in the middle of the diffusor width.

Each graph in Figure 15 gives the results of 2000 measurements superimposed on one impeller revolution. In this representation, the fluctuation from one revolution to the next appears as a vertical scattering. The results for three flow rates, chosen as examples, show clearly the flow disorganization at a critical flow rate of about 0.070 m^3/s, which appeared somewhat higher than that visualized at the impeller inlet.

Hot Wire Measurements in Air

In air, velocity measurements at the diffusor inlet (at about 10 mm from the impeller outlet) were made using a two hot-wire probe.

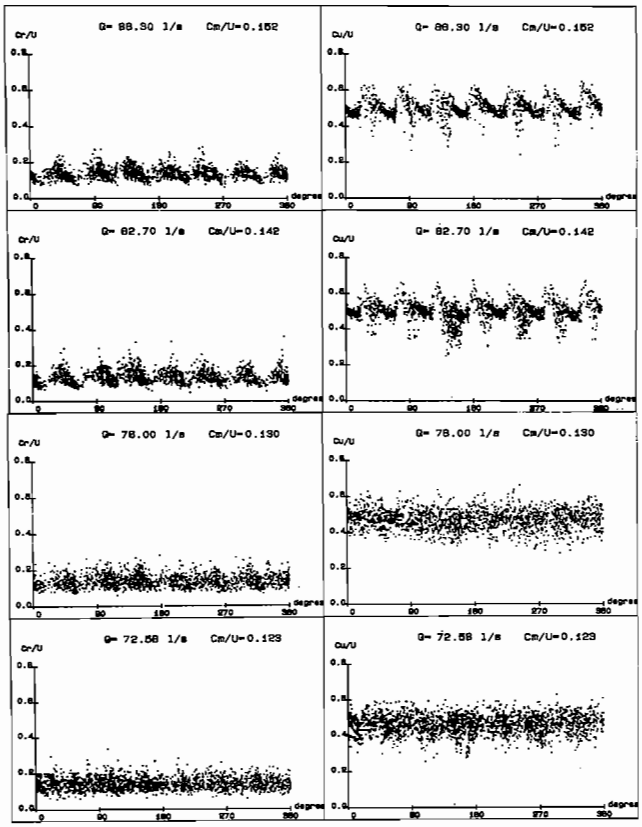

Figure 15. Absolute Velocity Profiles at Impeller Outlet from Laser Measurements (Water Tests).

A description of that technique was done by Desmet [6]. Electric signals from both wires were sampled by a numeric memory, transferred into a microcomputer and then translated into velocities (radial and circumferencial components). The measurements were made in the middle of the diffusor width, 5 mm from each wall. The evolution of velocity showed that when the flow rate was reduced, the radial component near the inlet shroud occasionally became negative. The velocity distributions (Figure 16) seemed to agree with the beginning of outlet reverse flow on the front shroud.

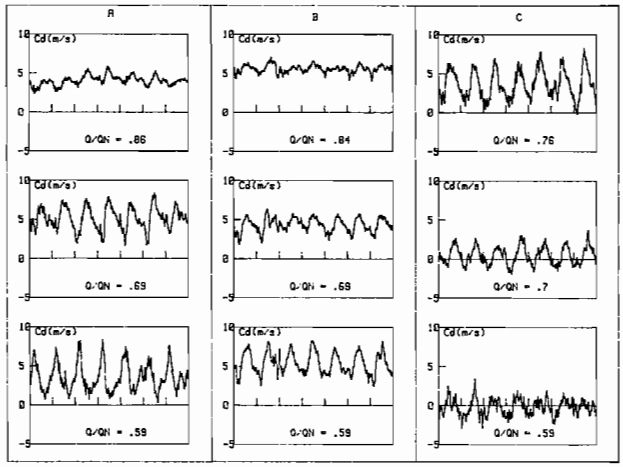

Figure 16. Velocity Radial Component Cd at Impeller Outlet from Hot Wire Measurements (Air Tests. A = 5 mm from Back Shroud. B = Channel Middle Line. C = 5 mm from Front Shroud.

INFLUENCE OF DIFFUSER DESIGN, LEAKAGE FLOW AND ROTATIONAL SPEED

Rotational Speed

In air, tests were made at three different speeds of rotation (Table 1) with varying Reynolds and Mach numbers. Pump performance changed very slightly. The visualized critical flow rate at the inlet was constant in all conditions, and the scattering was larger when looking at the outlet critical flow rate. The phenomena at outlet were more difficult to analyze with precision. The various results are summarized and presented in Table 4.

Table 4. Values of Critical Flow Rate Determined at Several Rotational Speeds.

Speed of rotation (rpm)	Q_K (inlet)/Q_N	Q_K (outlet)/Q_N
2500	0.67	0.78
2000	0.69	0.81
1700	0.68	0.78

Table 5: Variations of Leakage Flow.

Valves Setting (see Figure 3)		Leakage Flow Direction
V1	V2	
closed	closed	standard direction
connected with ambiant pressure (P1>P ATM)	closed	reverse leakage flow at impeller inlet
closed	connected with high pressure	reverse leakage flow at impeller outlet
connected with ambiant pressure (P1>P ATM)	connected with high pressure	reverse leakage flow at impeller inlet and outlet

Leakage Flow

A special design of labyrinths allowing some variations of the leakage flow at water impeller inlet and outlet is shown in Figure 3. Two intermediate annular chambers might be connected to external pressure conditions by means of a controlling valve. The variations obtained are presented in Table 5. The inlet critical flow rate appeared to be modified essentially in the case of an inlet leakage flow reversal, as is shown in Figure 17.

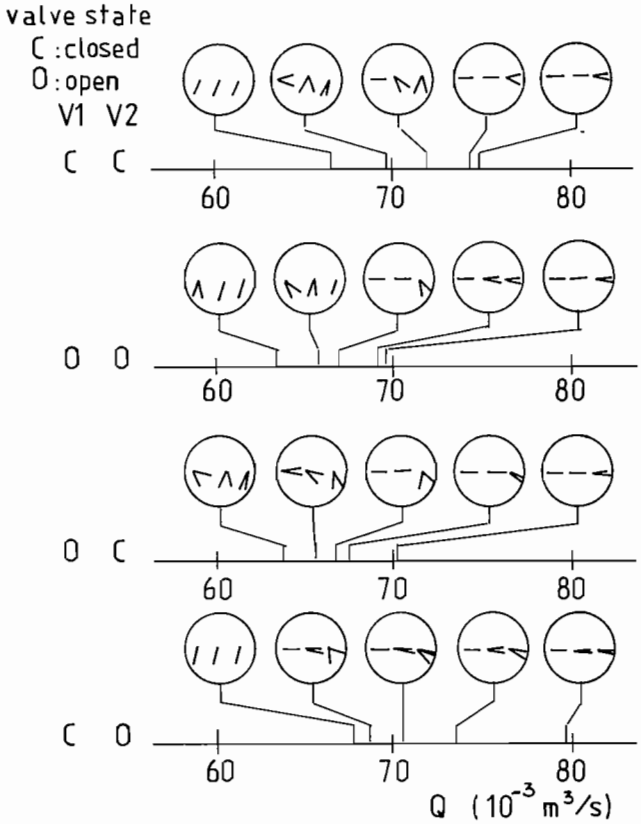

Figure 17. Influence of Leakage Flow on Reverse Flow Onset at Impeller Inlet (Water Tests).

Diffuser Width

Preliminary measurements in water were made with a wider diffuser (43 mm width instead of 30 mm in all other experiments). Results of these visualizations with threads on the inlet pipe wall are given in Figure 18. The maximum efficiency was naturally obtained for a larger flow rate, and the transition zone corresponding to reverse flow onset was broader than with the smaller diffuser.

Table 6: Values of Critical Flow Rate for Bladed and Vaneless Diffusers.

Speed of rotation (rpm)	Q_K (inlet)/Q_N		Q_K (outlet)/Q_N	
	6 blade diffuser	vaneless diffuser	6 blade diffuser	vaneless diffuser
2500	0.67	0.65	0.78	0.77
2000	0.69	0.64	0.81	0.73
1700	0.68	0.65	0.78	0.72

Vaneless Diffuser

In the air test-rig, tests were also made with a vaneless diffuser instead of the vaned diffuser used before. Table 6 gives the comparison of critical flow rates at inlet and outlet with both configurations. The relative critical flow rate appeared to be slightly lower with the vaneless diffuser.

Figure 19 shows the results of pressure fluctuations frequency analysis as already seen in Figure 14. The evolution of the amplitudes of fluctuations was quite different with the vaneless diffuser which shows the difficulty of interpreting such measurements.

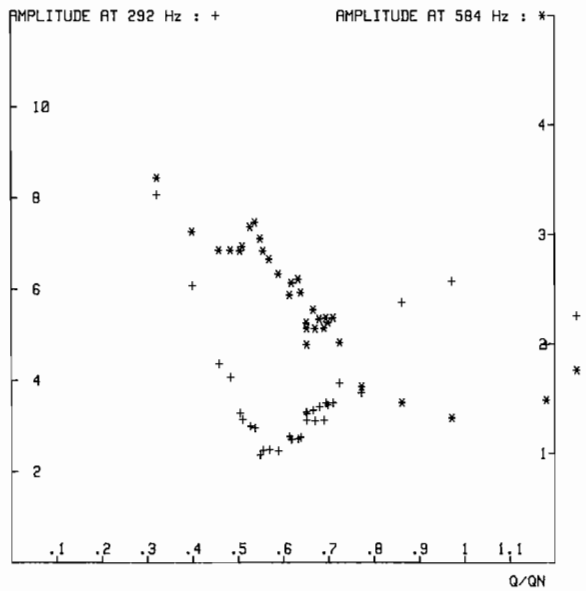

Figure 18. Water Test Pump Performance Curves (Broad Diffuser).

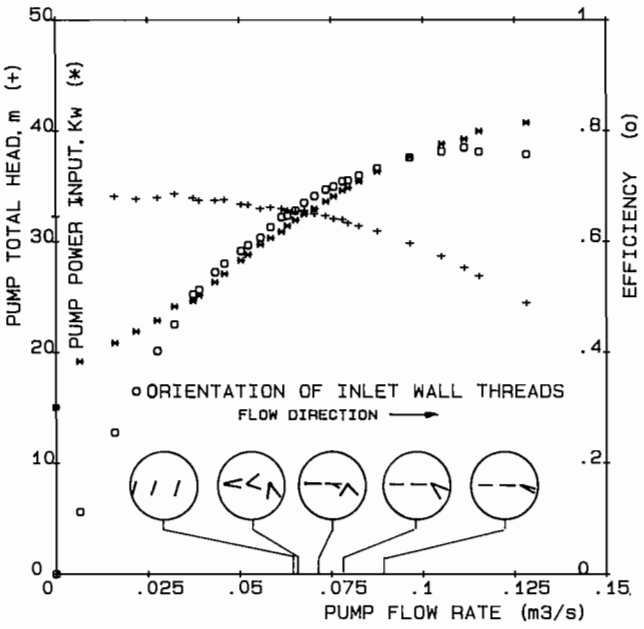

Figure 19. Pressure Fluctuation Analysis at Impeller Outlet with Vaneless Diffuser (Air Tests).

Table 7: General Comparison of Critical Flow Rates.

	WATER TESTS			AIR TESTS						FRASER FORMULA
	narrow diffuser	broad diffuser		bladed diffuser			vaneless diffuser			
	standard leakage flow	reversed inlet leakage flow		1700 rpm	2000 rpm	2500 rpm	1700 rpm	2000 rpm	2500 rpm	
Q_K inlet / Q_N	0.66	0.60	0.65	0.68	0.69	0.67	0.65	0.64	0.65	0.63
Q_K outlet / Q_N	From 0.68 To 0.72			0.78	0.81	0.78	0.72	0.73	0.77	0.63

DISCUSSION AND CONCLUSION

The results given in this paper, concerning the value of critical flow rate, are summarized in Table 7. They were completed with an analysis according to the Fraser correlation formula [1]. The principal conclusions which could be drawn from Table 7 are as follows:

The critical flow rate at the pump inlet appeared to be slightly higher in the air tests than in the water tests. This fact could be partly due to small inaccuracies in the flow measurements, but also, to the presence of a larger inlet leakage flow in air tests. Nevertheless, the order of magnitude was quite the same in both series of tests.

In the water tests as well as in air tests, the critical flow rate at the pump outlet was larger than the one found at the pump inlet. This fact was in contradiction with Fraser's formula.

In water tests, the reversal of inlet leakage flow lead to a much lower critical flow rate. On the contrary, a reversed outlet leakage flow rate did not seem to present a marked influence.

In air tests, the use of a vaneless diffuser lead to a critical flow rate slightly lower than with a bladed diffuser.

The influence of the speed of rotation was not well marked in air tests.

Direct determination of the critical flow rate from visualization gave rather well defined values. The use of indirect methods, such as those based on impeller head input measurements (Figures 11a and 12a), on impeller power input (Figures 11b and 12b), on pressure fluctuations analysis (Figures 14 and 19) lead to a much higher uncertainty.

Determination of the critical flow rate at the impeller outlet was more delicate than at the impeller inlet. For that reason, methods more sophisticated than visualization threads should be used. Results from hot wire measurement appeared quite satisfactory (Figure 16) with improvement needed in the laser measurements (Figure 15).

Complementary tests are now going on in order to complete these preliminary results and to check, more particularly, the following points:

- location of stalling region at impeller outlet. The stall was found near front shroud in air impeller but not well defined in water impeller.
- influence of leakage flow rate in air tests.
- influence of volute casing width.

REFERENCES

1. Fraser, W. H., "Recirculation in Centrifugal Pumps," World Pumps, *188*, pp. 227-235 (1982).
2. Schiavello, B., "Critical Flow Engendering Appearance of Recirculation at Centrifugal Pump Impeller Inlet: Determinant Phenomena, Detection Methods, Forecasting Criteria," La Houille Blanche, pp. 139-158 (2-3-1982).
3. N.F.X10.102 Standard, "Measurement of Fluid Flow by Means of Orifice Plates, Nozzles and Venturi Tubes. First Part: Primary Elements Inserted in Circular Cross-section Conduits."
4. N.F.X10.104 Standard, "Measurement of Fluid Flow by Means of Orifice Plates, Nozzles and Venturi Tubes. Guide for Practical Use."
5. Rey, R., Guiton, P. Kermaric, Y., Vullioud, G., "Statistical Study of Partial Flow Characteristics of Centrifugal Pumps and of Approximate Determination of the Critical Flow," La Houille Blanche, pp. 107-120 (2-3-1982).
6. Desmet, B., "Pressure and Speed Measurements in a Centrifugal Fan (Rotor and Stator) Before and After the Appearance and Disappearance of Rotating Stalls," La Houille Blanche, pp. 167-174 (2-3-1982).

ACKNOWLEDGEMENTS

This study has received financial support from the French Ministry of Industry and Research under grant n° DGRST 81-S-0882 and from the following companies: Bergeron S.A., Metraflu, Neyrpic.

The authors wish to acknowledge all the members of the working group of Societe Hydrotechnique de France for their contribution.